RSC Advances

ROYAL SOCIETY OF CHEMISTRY

www.rsc.org/advances

Facile synthesis of single-crystalline α-Fe_2O_3 hollow nanospheres with gas sensing properties

Pei-Pei Wang,[a] Xiao-Xin Zou,[a] Liang-Liang Feng,[a] Jun Zhao,[a] Pan-Pan Jin,[a] Rui-Fei Xuan,[b] Ye Tian,[c] Guo-Dong Li[a] and Yong-Cun Zou*[a]

High-quality single-crystalline hollow α-Fe_2O_3 nanospheres were prepared, using ZnS-CHA nanohybrid as additive with gas sensing property.

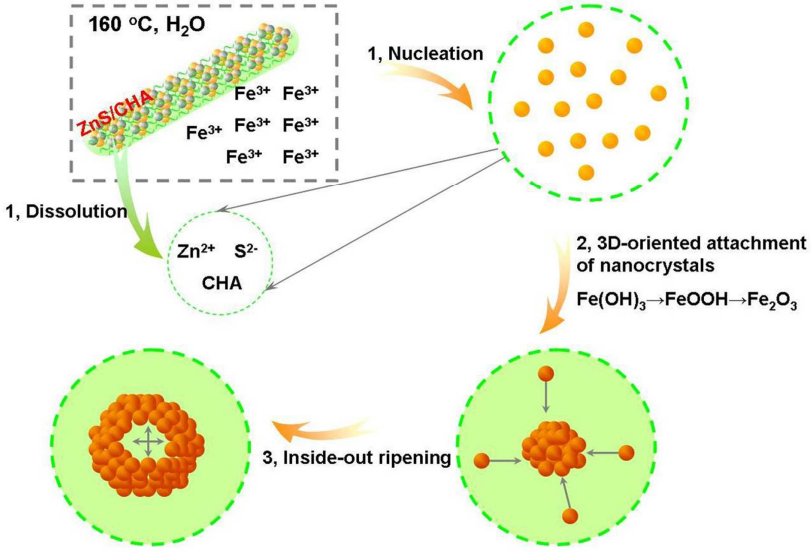

Cite this: DOI: 10.1039/c0xx00000x

www.rsc.org/xxxxxx

ARTICLE TYPE

Facile synthesis of single-crystalline hollow α-Fe_2O_3 nanospheres with gas sensing property

Pei-Pei Wang,[a] Xiaoxin Zou,[a] Liang-Liang Feng,[a] Jun Zhao,[a] Pan-Pan Jin,[a] Rui-Fei Xuan,[b] Ye Tian,[c] Guo-Dong Li[a] and Yong-Cun Zou*[a]

Received (in XXX, XXX) Xth XXXXXXXXX 20XX, Accepted Xth XXXXXXXXX 20XX
DOI: 10.1039/b000000x

High-quality single-crystalline hollow α-Fe_2O_3 nanospheres were prepared, using the ZnS-CHA (CHA = cyclohexylamine) nanohybrid as an additive through solvothermal reaction, which avoid of tedious steps and high temperature calcination process. The formation process of these hollow nanospheres can be divided into two stages: i) formation of solid Fe_2O_3 nanospheres and ii) preferential inside-out dissolution of the solid nanoparticles to form hollow nanospheres. Due to the unique single-crystalline hollow structure, the as-obtained α-Fe_2O_3 nanomaterial exhibits enhanced gas sensing property.

As an important n-type semiconductor, α-Fe_2O_3 has been widely studied for its comprehensive applications such as gas sensors, Li-ion batteries, pigments, magnetic recorders and catalysts.[1-11] Considerable research efforts have been devoted to develop methods to delicate control over the morphology, size and functions of α-Fe_2O_3. Most of the reported work evolves around methodologies of constructing hollow or single-crystalline Fe_2O_3,[2,5,12-19] among which single-crystalline hollow Fe_2O_3 was the best representative.[17,20] The first single-crystalline hollow Fe_2O_3 was reported by Eswaramoorthy's group, using carbonaceous spheres as sacrificial templates with a sol-gel process. The single-crystalline hollow spheres were homogeneous, but they were collected by high tempreature post-calcination which was a bit energy consumption.[5] Fan and his coworkers reported a shape-controlled method making hollow single-crystalline Fe_2O_3 by hydrothermal treatment at 220 ^oC for 60 h, which process was easy to realize but a bit time-consuming.[21] Combining the functionality of Fe_2O_3 with its single-crystalline hollow structure is of essential for function optimum. Quest for simple, controllable and scalable synthesis of single-crystalline hollow Fe_2O_3 materials have been obtained tremendous attention.

In this paper, we report a facile template-free approach to prepare single-crystalline hollow Fe_2O_3 with ZnS-CHA nanohybrid as an additive. The procedure was conducted without post-high tempreature calcination process within 24 h. The hollow nanospheres are in diameters of 200-300 nm with well-defined shape and size, and the size of the shells are around 20-50 nm. And the as-obtained Fe_2O_3 exhibits promising chemical sensing properties. The hollow single-crystalline α-Fe_2O_3 nanospheres show good gas sensing property towards ethanol, and exhibits good response characteristics towards multiple of target gases. As the raw material, ZnS-CHA nanocomposite, was easy to sale up, the current contribution may offer a versatile approach for the development of a series of metal oxide for advanced applications.

Fig. 1A shows the SEM image of the single-crystalline Fe_2O_3 with hollow spheres in uniformed size, and the hollow structure was further determined by TEM analysis, which exhibits the diameter in the range of 200-300 nm with wall thickness around 20-50 nm (Fig. 1B). High resolution TEM (HRTEM) show the particles with continuous lattice fringes measured from (101) plane to be 0.42 nm and (006) plane to be 0.23 nm in (Fig. 1C), and the selected area electron diffraction (SAED) pattern (Fig. 1D) evidently gives the single-crystalline nature of the nanospheres.

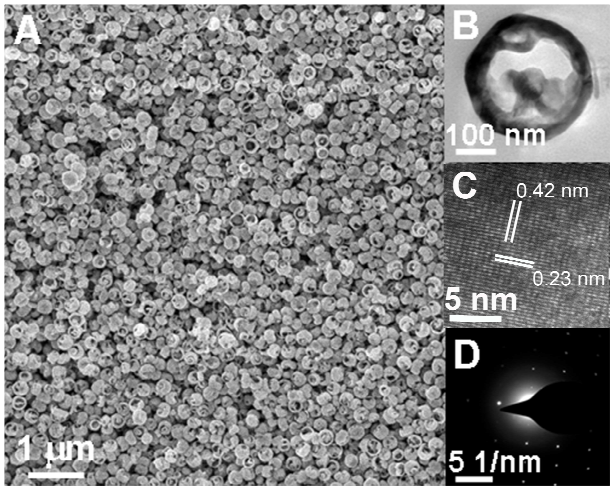

Fig. 1 (A) SEM; (B) TEM; (C) HRTEM images and (D) SAED pattern of the obtained single-crystalline α-Fe_2O_3 nanospheres.

High-quality single-crystalline hollow α-Fe_2O_3 nanospheres were prepared using ZnS-CHA nanohybrid as an additive. In the typical system, zinc acetate dihydrate and thiourea functioned as the zinc source and the sulfur source, respectively, whereas cyclohexylamine (CHA) acted as both the solvent and the reactive agent. In comparison with the previous synthetic condition of ZnS-CHA, we just decreased

the concentration of the zinc source (75 mmol/L in referenced paper and 37.5 mmol/L in this paper) in the reaction mixture to get a high-quality ZnS-CHA sample, while maintaining the molar ratio of zinc to sulfur (1:2). The structure of as-prepared ZnS-CHA was similar to that in the previous report, as demonstrated by powder X-ray diffraction (XRD), infrared spectroscopy (IR), and X-ray photoelectron spectroscopy (XPS) (see Fig. S1† in the Supplementary information). The ZnS-CHA nanocomposite was formed from the very small ZnS nanoparticles through assembly with the CHA molecules. The zinc and sulfur species were Zn^{2+} and S^{2-}, respectively, and the CHA molecules were not protonated in the ZnS-CHA nanocomposite. Based on the thermogravimetric (TG) result (Fig. S1C†), the empirical composition of the as-prepared ZnS-CHA nanocomposite was close to ZnS·CHA, in which the amount of CHA was obviously higher than that reported previously, probably due to the higher CHA : Zn ratio in this reaction condition. In addition, the morphology of the as-prepared ZnS-CHA with a short rod-shape (see SEM image in Fig. S2†) was also different from that reported previously (irregular powder sample).[22] It should be noted that, the exact crystal structure was still not available since the large single crystal of ZnS-CHA can't be obtained. Regardless of its exact crystal structure, ZnS-CHA has been applied as an efficient precursor for the preparation of inorganic nanosheet material.[23] It was also used as a novel additive for formation of the well-defined α-Fe_2O_3 nanospheres, as demonstrated as below.

In order to understand the formation process of the uniform hollow α-Fe_2O_3, time-dependent experiments were carried out carefully on basis of the above experimental procedures. At given time interval, the powder products were harvested by centrifuging and washing with deionized water for further characterization. Corresponding SEM photographs were shown in Fig. S3†. As shown in the pictures, the nanoparticles were so small that we couldn't see them clearly during 1 h (Fig. S3A†). After that, the solid products we collected were with diameters in the range of 200-300 nm (Fig. S3B,C†). It does't form the completely hollow nanospheres until 24 h later (Fig. S3E, F†), and the diameters of the nanospheres were not changed obviously. The schematic diagram for formation of the hollow nanosphere was shown in Scheme S1†. Based on the above results, the formation process of these hollow nanospheres can be mainly divided into two stages: i) formation of solid Fe_2O_3 nanospheres and ii) preferential inside-out dissolution of the solid nanoparticles to form hollow nanospheres.

$$Fe^{3+} + H_2O \rightarrow Fe(OH)_3 / FeOOH + H^+ \quad (1)$$

$$Fe(OH)_3/FeOOH \rightarrow Fe_2O_3 + H_2O \quad (2)$$

Under a hydrothermal reaction condition, the formation of Fe_2O_3 nanoparticles from Fe^{3+} ions is based on the equations 1 and 2. Then the 3-D oriented attachment of nanocystals was formed,[4,5,24] the nanocystals began to self-assembly well-defined single-crystalline α-Fe_2O_3 soild nanospheres. Accompanying this process, the pH value of the reaction system will decrease due to the generation of protons (equation 1; The pH value of the fianl reaction system is as low as 2.4). This is will provide an acidic condition to dissolve the ZnS-CHA hybrid and to selectively inside-out dissolve the solid Fe_2O_3 nanospheres because the inner part was less stable compared with the outer surface layer of Fe_2O_3 nanocrystal.[5,25] At last, the hollow single-crystalline nanospheres were formed.

XRD patterns were shown in Fig. 2A. It was clear that the product was consists of α-Fe_2O_3 and ZnS at 1 h, and the pure α-Fe_2O_3 (JCPDS card No: 33-0664) with no impure peaks was formed after 6 h. The product we obtained after 24 h was in good crysatlline with narrow peaks and smooth base line. Raman spectra was also carried out to determine the crystal phase and crystalline condition (Fig. 2B). The characteristics roman bands were typical α-Fe_2O_3. The base lines of the products in 1 h and 6 h were a bit rough revaling the low crystalline. At last, the hollow Fe_2O_3 in better quality crystalline was obtained after 24 h. The Raman spectra matched very well with the XRD patterns.

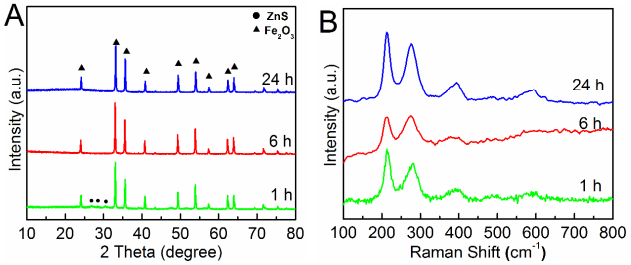

Fig. 2 (A). XRD patterns and (B). Raman spectra of the α-Fe_2O_3 nanospheres obtained at 1 h, 6 h and 24 h.

Surface elements of the hollow nanoshperes were examined by XPS spectra shown in Fig. S4. High-resolution of Fe $2p_{1/2}$ and Fe $2p_{3/2}$ peaks of the hollow α-Fe_2O_3 (Fig. S4A†) were located at 725.3 and 711.2 eV, respectively. The shakeup satellite at 719.9 eV was the typical Fe^{3+} in Fe_2O_3.[4,8] High-resolution of O 1s was shown in Fig. S4B†. The vibrations of crystal lattice O occupied nearly 82.8 %, and the adsorption of molecule oxygen takes only 27.2 %.

In order to determine the role of ZnS-CHA nanohybrid in formation of the well-defined single-crystalline hollow α-Fe_2O_3, four different control experiments were performed for comparative studies. (1) The first control experiment involved the synthesis of materials with no ZnS-CHA being used as the above synthetic procedure, this resulted in only uneven α-Fe_2O_3 nanoparticles formed with average size of ~ 300 nm (Fig. S5A†). The product we collected in this process was called Fe_2O_3-1; (2) Instead of ZnS-CHA, the same amount of pure CHA (0.015 g) was used under identical reaction conditions. However, the synthesis also resulted in irregular α-Fe_2O_3 nanoparticles with average size of ~ 100 nm (Fig. S5B†) which was called Fe_2O_3-2; (3) Treating the ZnS-CHA nanocomposite at 160 °C in water solution to synthesis the pure ZnS, and then taking the same amount of ZnS instead of the ZnS-CHA nanohybrid, the final product was also uneven α-Fe_2O_3 nanoparticles with average size of ~ 300 nm (Fig. S5C†) which was called Fe_2O_3-3; (4) The as prepared pure ZnS (0.015 g) with pure CHA (0.015 g) were used to react at the same condition as mentioned above, without exception,

the final product was also uneven nanoparticles with average size of ~ 100 nm (Fig. S5D†) named as Fe_2O_3-4. Therefore, we can conclude that the ZnS-CHA nanohybrid plays an essential role in preparation of the well-defined single-crystalline hollow α-Fe_2O_3 nanospheres.

To further confirm the relationship between the iron content with the single-crystalline hollow Fe_2O_3, controlled experiments were conducted by using 0.32 g, 0.48 g and 0.64 g $FeCl_3{\cdot}6H_2O$. As a result, the obtained Fe_2O_3 nanospheres were polycrystalline with increased diameters and the corresponding SEM images were given in Fig. S6†.

Gas sensing performance was employed by a CGS-8 gas sensing measurement system (Beijing Elite Tech Company Limited). The whole process was the same as mentioned before.[26-28] Sensitivity was designed as *Ra/Rg*, where *Ra* was the resistance of sensors in air, *Rg* was the resistance of the sensors in the target gases.[9,29,30] Gas sensing properties of the single crystal hollow α-Fe_2O_3 nanospheres were researched towards ethanol. The concentration-sensitivity relationship experiments were executed from 5 ppm to 2000 ppm at 300 °C (Fig. 3A). The sensitivity was increased with incresing the concentration of ethanol. Excepting the sensitivity, there were also some vital parameters for the snesing materials, such as response time, recovery time and the stability. The magnification curve of the single-crystalline hollow Fe_2O_3 towards 500 ppm ethanol was shown in Fig. S9†. The response time was defined as the time from *Ra* to *Ra* - 90% × (*Ra*-*Rg*), and the recovery time was defined as the time from *Rg* to *Rg* + 90% × (*Ra*-*Rg*). The single-crystalline hollow Fe_2O_3 exhibits short respons time for 5 s and fast recovery time for 2 s, both of which were much better than the reported sesults.[16,31] The dynamic response curves of the contrast Fe_2O_3-1 mentioned above (control experiment (1)) to ethanol was shown in Fig. 3B. Concentration-response curves of the two sensors were shown in Fig. 3C. The single-crystalline hollow Fe_2O_3 shows the superior response towards ethanol compared to contrast Fe_2O_3-1 shown in Fig. 3D. The single-crystalline hollow Fe_2O_3 also gives higher response to other gases such as acetone, methanol, and formaldehyde than the contrast Fe_2O_3-1. In order to estimate the stablity of the single-crystalline hollow Fe_2O_3, time depended gas sensing experiments were taken every one day for ten days. Slight variations were found duiring the ten days measurement towards 5, 500 and 2000 ppm ethanol (Fig. S10†). This results give the final conclusion that the sensors exhibit good repeatability to ethanol.

The sensing mechanism of Fe_2O_3 sensors was the same as the traditional semiconductor sensors. The main mechanism was based on the reaction between the deteceted gas molecules and the chemisorbed oxygen species on Fe_2O_3 surface. The Fe_2O_3 sensors will exhibits a relatively high resistance state by generate O^{2-} or O^- in the air condition,[32] since the adsorbed oxygen molecules will capture electrons from the Fe_2O_3 layer (conduction band of the Fe_2O_3). When the target reductive gases were introduced at an moderate operating temperature (*e.g.*, ethanol), the Fe_2O_3 surface layer oxygen species will have a reaction with them, and then the electrons will be given back into the Fe_2O_3 layer, giving rise to the reduced surface oxygen species along with the decreased surface resistance. The reaction equation was presented as follows:

$$C_2H_5OH + 6O^- \leftrightarrow 2CO_2 + 3H_2O + 6e^- \quad (3)$$

The enhanced sensing performance may attribute to the hollow structure of the single-crystalline Fe_2O_3. TEM and HRTEM images of Fe_2O_3-1 were shown in Fig. S7†, which further confirmed its solid structure. Single-crystalline hollow Fe_2O_3 owns larger BET surface area, the BET surface area of the single-crystalline hollow Fe_2O_3 was 31 $m^2\ g^{-1}$ (Fig. S8A†), remarkably higher than that of the Fe_2O_3-1 (Fig. S8B†, 12 $m^2\ g^{-1}$). The hollow structure with higher surface to volume ration could provide more active sites for gas molecules adsorption, leading to the higher sensitivity and shorter response-recovery times. The sparse physiognomy make the single-crystalline hollow Fe_2O_3 nanospheres a good candidate for high performance sensing material.

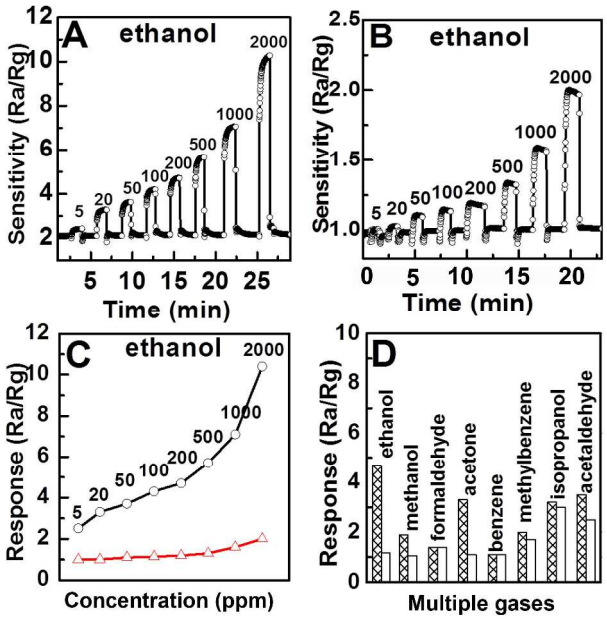

Fig. 3 Gas sensing property toward 5-2000 ppm ethanol of (A) the single-crystalline Fe_2O_3 and (B) the Fe_2O_3-1; (C) Concentration-response curves of the single-crystalline Fe_2O_3 (○) and the Fe_2O_3-1 (△) towards ethanol; and (D) Response of the single-crystalline Fe_2O_3 (criss-crossed rectangle) and the Fe_2O_3-1 (open rectangle) towards multiple gases.

Conclusion

Single-crystalline hollow hematite (Fe_2O_3) nonospheres were synthesized through template-free solvothermal reaction, without surfactant and high temperature calcination process. The diameters of the nanospheres were arond 200-300 nm with uniform shape and size. The shells of the spheres were on the nanoscale around 20-50 nm. The ZnS-CHA nanohybrid, which used as the source material, plays a necessary role in preparation of the uniform single α-Fe_2O_3 nanospheres. The hollow nanospheres show good gas sensing property towards ethanol. This method provides us an easy and convenient way to synthesize single crystalline hollow nanospheres.

Acknowledgement

This work was supported by the National Natural Science Foundation of China (21371070); Science and Technology Development Projects of Jilin Province (20140101041JC, 20130204001GX); Natural Science Foundation of Tianjin, China (12JCYBJC14000).

Notes and references

[a]*State Key Lab of Inorganic Synthesis & Preparative Chemistry, College of Chemistry, Jilin University, Changchun 130012, P. R. China Fax: 86-431-85168624; Tel: 86-431-85168318; E-mail: zouyc@jlu.edu.cn;*
[b]*College of Materials Science and Engineering, China University of Mining and Technology, Xuzhou 221116, China;*
[c]*Tianjin Key Laboratory of Applied Catalysis Science and Technology, School of Chemical Engineering, Tianjin University, Tianjin 300072, China.*

†Electronic Supplementary Information (ESI) available: [characterization details of the ZnS-CHA nanocomposite, SEM and TEM of the relevant Fe_2O_3 products].

1. H.-J. Song, X.-H. Jia, H. Qi, X.-F. Yang, H. Tang and C.-Y. Min, *J. Mater. Chem.*, 2012, **22**, 3508.
2. B. Wang, J. S. Chen, H. B. Wu, Z. Wang and X. W. Lou, *J. Am. Chem. Soc.,* 2011, **133**, 17146.
3. L. Xu, J. Xia, K. Wang, L. Wang, H. Li, H. Xu, L. Huang and M. He, *Dalton Trans.*, 2013, **42**, 6468.
4. X. Hu, J. C. Yu, J. Gong, Q. Li and G. Li, *Adv. Mater.*, 2007, **19**, 2324.
5. D. Jagadeesan, U. Mansoori, P. Mandal, A. Sundaresan and M. Eswaramoorthy, *Angew Chem. Int. Ed.*, 2008, **47**, 7685.
6. H.-J. Kim, K.-I. Choi, A. Pan, I.-D. Kim, H.-R. Kim, K.-M. Kim, C. W. Na, G. Cao and J.-H. Lee, *J. Mater. Chem.*, 2011, **21**, 6549.
7. D. Chen, W. Wei, R. Wang, J. Zhu and L. Guo, *New J. Chem.*, 2012, **36**, 1589.
8. T. Wang, S. Zhou, C. Zhang, J. Lian, Y. Liang and W. Yuan, *New J. Chem.,* 2014, **38**, 46.
9. P. Sun, Z. Zhu, P. Zhao, X. Liang, Y. Sun, F. Liu and G. Lu, *CrystEngComm,* 2012, **14,** 8335.
10. N. V. Long, Y. Yang, M. Yuasa, C. M. Thi, Y. Cao, T. Nann and M. Nogami, *RSC Adv.*, 2014, **4**, 8250.
11. L. Zhang, H. B. Wu, R. Xu and X. W. Lou, *CrystEngComm*, 2013, **15**, 9332.
12. M. Cao, T. Liu, S. Gao, G. Sun, X. Wu, C. Hu and Z. L. Wang, *Angew Chem. Int. Ed.*, 2005, **44**, 4197.
13. H. Deng, X. Li, Q. Peng, X. Wang, J. Chen and Y. Li, *Angew. Chem.,* 2005, **117**, 2842.
14. B. Lv, Z. Liu, H. Tian, Y. Xu, D. Wu and Y. Sun, *Adv. Funct. Mater.,* 2010, **20**, 3987.
15. X. Liu, J. Zhang, S. Wu, D. Yang, P. Liu, H. Zhang, S. Wang, X. Yao, G. Zhu and H. Zhao, *RSC Adv.*, 2012, **2**, 6178.
16. X. Li, W. Wei, S. Wang, L. Kuai and B. Geng, *Nanoscale,* 2011, **3**, 718.
17. B. Lv, Y. Xu, D. Wu and Y. Sun, *Chem. Comm.*, 2011, **47**, 967.
18. N. K. Chaudhari, H. Chan Kim, D. Son and J.-S. Yu, *CrystEngComm*, 2009, **11**, 2264.
19. S. Bharathi, D. Nataraj, M. Seetha, D. Mangalaraj, N. Ponpandian, Y. Masuda, K. Senthil and K. Yong, *CrystEngComm*, 2010, **12**, 373.
20.W. Wu, R. Hao, F. Liu, X. Su and Y. Hou, *J. Mater. Chem. A*, 2013, **1**, 6888.
21. H. Fan, G. You, Y. Li, Z. Zheng, H. Tan, Z. Shen, S. Tang and Y. Feng, *J. Phys. Chem. C*, 2009, **113**, 9928.
22. X. X. Zou, G. D. Li, J. Zhao, P. P. Wang, Y. N. Wang, L. J. Zhou, J. Su, L. Li and J. S. Chen, *Inorg. chem*. 2011, **50**, 9106.
23. Y. Yu, J. Zhang, X. Wu, W. Zhao and B. Zhang, *Angew Chem. Int. Ed.,* 2012, **51**, 897.
24. L.-P. Zhu, H.-M. Xiao, W.-D. Zhang, G. Yang and S.-Y. Fu, *Cryst. Growth Des*., 2008, **8**, 957.
25. X.Wu, Y. Yu, Y. Liu, Y. Xu, C. Liu, B. Zhang, *Angew. Chem. Int. Ed.*, 2012, **51**, 1.
26. P.-P. Wang, Q. Qi, X. Zou, J. Zhao, R.-F. Xuan and G.-D. Li, *RSC Adv*., 2013, **3**, 23980.
27. J. Zhong, C. Cao, Y. Liu, Y. Li and W. S. Khan, *Chem. Commun*., 2010, **46**, 3869.
28. J. Zhao, X. Zou, L.-J. Zhou, L.-L. Feng, P.-P. Jin, Y.-P. Liu and G.-D. Li, *Dalton Trans*., 2013, **42**, 14357.
29. C. Zhao, G. Zhang, W. Han, J. Fu, Y. He, Z. Zhang and E. Xie, *CrystEngComm*, 2013, **15**, 6491.
30. X.-X. Zou, G.-D. Li, P.-P. Wang, J. Su, J. Zhao, L.-J. Zhou, Y.-N. Wang and J.-S. Chen, *Dalton Trans.*, 2012, **41**, 9773.
31. Q. Hao, S. Liu, X. Yin, Z. Du, M. Zhang, L. Li, Y. Wang, T. Wang, Q. Li, *CrystEngComm*, 2011, **13**, 806.
32. J. Y. Liu, Z. Guo, F. L. Meng, Y. Jia, T. Luo, M. Q. Li, J. H. Liu, *Cryst. Growth Des*., 2009, **9**, 1716.

